

RESEARCH PAPER

Zinc amino acid chelate and the Aryl Hydrocarbon Receptor (AHR) cooperate in improving the barrier function of a Caco-2 cell intestinal epithelium

Xiuchuan Hu^a, Rui Wang^a, Peter Kille^b, Wolfgang Maret^a, Christer Hogstrand^{c,*}

^a Department of Nutritional Sciences, School of Life Course and Population Sciences, King's College London, London, UK

^b School of Biosciences, Cardiff University, Cardiff, UK

^c Department of Analytical, Environmental and Forensic Sciences, School of Cancer and Pharmaceutical Sciences, King's College London, London, UK

Received 12 August 2024; received in revised form 20 March 2025; accepted 21 March 2025

Abstract

Zinc and several physiologically relevant ligands of the aryl hydrocarbon receptor (AHR) are nutrients that promote intestinal barrier function. We have identified that AHR activation upregulates the expression of zinc importers in the intestinal epithelium to increase intracellular zinc concentrations, which leads to improved epithelial barrier function. Here, we investigated if an amino acid chelate of zinc, in cooperation with AHR activation, can improve the barrier function of a differentiated Caco-2 cell epithelium. Functional assays of the Caco-2 cell epithelium demonstrate that both ZnSO₄ and a lysine and glutamic acid chelate of Zn, in combination with the physiological AHR agonist 6-formylindolo[3,2-b]carbazole (FICZ), increase expression of tight junction proteins at the mRNA and protein levels. FICZ increases uptake of zinc into the epithelium in the presence of ZnSO₄ or the amino acid Zn chelate in the medium to equal extents. We conclude that the lysine and glutamic acid chelate of Zn is as efficacious as ZnSO₄ in reducing permeability of the Caco-2 cell epithelium in the presence of FICZ. The results suggest that dietary supplementation with bioavailable forms of zinc together with nutritional AHR agonists may be beneficial in improving gut barrier function and help prevent inflammatory bowel disease (IBD).

© 2025 The Authors. Published by Elsevier Inc.

This is an open access article under the CC BY license (<http://creativecommons.org/licenses/by/4.0/>)

Keywords: Amino acid chelate of zinc; Organic zinc; Aryl hydrocarbon receptor, AHR; Inflammatory bowel disease, IBD; Colitis; Crohn's disease.

1. Introduction

The main functions of the intestinal epithelium barrier are to selectively allow the passage of nutrients while separating the intestinal epithelial cells from other gut contents, thereby protecting against attacks from pathogenic bacteria, fungi, viruses, antigens, and other harmful agents [1–3].

Both the aryl hydrocarbon receptor (AHR) and zinc play roles in maintaining the integrity of the intestinal epithelium. The AHR is a nuclear receptor belonging to the basic helix–loop–helix–PER–ARNT–SIM ((bHLH–PAS)) family of transcription factors [4]. Nutritional agonists of AHR, including indoles and tryptophan metabolites, are mainly found in cruciferous vegetables, such as broccoli [5].

AHR signalling is important for the immune system. AHR activation can recruit immune cells to the intestine, aiding in immune regulation and reducing inflammation, such as through IL-10 gene expression [6–8]. AHR is also essential for the survival

and function of certain immune cell populations, including type 3 innate lymphoid cells, T helper 17 cells, and double-positive CD4+CD8 $\alpha\alpha$ + intraepithelial lymphocytes [7–12]. Conditions like IBD are exacerbated in mice where AHR signalling is lost [11,13,14].

AHR also aids the intestinal barrier function independent of the immune system [13,14]. Activation of AHR with indole-3-carbinol increased the expression of mucin (MUC2) in mice small intestinal organoids and the number of goblet cells *in vivo* [15,16]. Goblet cells play a crucial role in gut barrier function by providing the mucous layer [17]. Besides its role in the regulation of both innate and adaptive immune responses [18], zinc can regulate the gut epithelial barrier by promoting formation of tight junctions [19]. This may explain why zinc supplementation is widely used to prevent diarrhoea in children as well as in farm animals [20]. A recent study showed that upon activation by the endogenously produced AHR agonist, 6-formylindolo[3,2-b]carbazole (FICZ), AHR transcriptionally stimulates expression of several zinc importers of the SLC39 family members to increase zinc influx resulting in downstream enhancement of tight junction (TJ) protein abundance [14].

Zinc participates in the regulation of virtually every aspect of biology, including fertilization, cell division, differentiation,

* Corresponding author at: Franklin-Wilkins Building, 150 Stamford Street, London, SE1 9NH UK.

E-mail address: christer.hogstrand@kcl.ac.uk (C. Hogstrand).

growth, immunity, retinal epithelium function, and cognition [19–22]. However, most studies on such roles of zinc are based on inorganic zinc salts such as ZnSO₄ rather than zinc chelates, which are becoming increasingly popular as zinc supplements. ProPath[®] Zn is an amino acid chelate of zinc containing lysine and glutamic acid, each binding with a separate zinc ion. It has been approved as a safe and efficacious zinc source for animals [23–25]. In this study, we assessed the ability of ProPath[®] Zn to promote barrier function of a Caco-2 cell epithelium in the presence of FICZ.

2. Materials and methods

2.1. Zinc sources

ZnSO₄ · 7H₂O was from Sigma-Aldrich (Z0251). ProPath[®]Zn, and ProPath[®] amino acids were provided by Zinpro[®]. ProPath[®] Zn comprises a 1:1 molar combination of zinc DL-lysine (Zn-C₆H₁₄N₂O₂) and zinc DL-glutamate (Zn-C₅H₈NO₄Na), and the ProPath[®] amino acids (Lys-HCl-MSG · H₂O) consists of DL-lysine (C₆H₁₄N₂O₂) and DL-glutamate (C₅H₈NO₄Na) with 1 to 1 molar ratio. Total zinc contents of both compounds were confirmed with Inductively coupled plasma mass spectrometry (ICP-MS) (see 4.10 below).

2.2. Cell line and culture

Human epithelial colorectal adenocarcinoma adherent Caco-2 cells, generously provided by Prof. Paul Sharp of King's College London, were cultured in Minimum Essential Medium Eagle (MEM, Cat: M4655-500ML, Merck). The culture medium, MEM, was supplemented with 10% v/v nonheated fetal bovine serum (FBS, Cat: F7524-500ML, Merck), 1% v/v 100 × MEM non-essential amino acid solution (Merck), 1% v/v 250 µg/mL Amphotericin B (Merck), and 1% v/v 100 units/ml penicillin (Merck). The cells were maintained at 37°C in a humidified atmosphere of 95% air and 5% CO₂. Cells from passages 25–31 were utilized, and passaging was performed by treatments with 1 × 0.25% trypsin-EDTA (Fisher Scientific) after washing by phosphate buffered saline (PBS) with passage intervals of 4 days. The cells were grown in the inserts of a 24-well plate for more than 2 weeks. Upon reaching a trans-epithelial electrical resistance (TEER) exceeding 400 Ω × cm², the cells underwent differentiation, exhibiting characteristics akin to enterocytes of the small intestine, as previously described [26–29]. The protocol reproducibly generates a differentiated epithelium as evidenced by an increase in villin protein and Divalent Metal Transporter-1 (DMT1) protein and mRNA expression (markers of enterocyte differentiation), and a decrease in transferrin receptor protein (indicative of decreased cell proliferation) [29]. These changes in gene and protein expression were accompanied by an increase in iron absorption, which is only observed in mature enterocytes, adding to the weight of evidence for the functional differentiation and maturation of the cells to express an enterocyte-like phenotype [29].

2.3. RNA extraction

TRIzol Reagent (Cat: 15596026, Thermo Fisher Scientific) was employed for the extraction of total RNA, with subsequent treatment using DNase I (Cat: 10229144, Fisher Scientific) to eliminate any residual DNA. The purified RNA was obtained either by employing RNAClean XP Beads (Cat: A63987, Beckman Coulter), or utilizing the RNAdvance Tissue RNA Isolation kit (Cat: A32649, Beckman Coulter). Following extraction, the RNA samples were then assessed for purity and quantity using a Nanodrop ND-1000 microlitre spectrophotometer.

2.4. cDNA synthesis

cDNA synthesis was prepared from the total RNA of cells using High-Capacity RNA-to-cDNA Kit (Cat: 10400745, Fisher Scientific) supplemented with 1 U RNase Inhibitor (Cat: 10615995, Fisher Scientific).

2.5. Quantitative real-time PCR (qPCR)

qPCR assays were designed using the online Universal Probe Library (UPL) assay design tool (https://lifescience.roche.com/en_gb/brands/universal-probe-library.html#assay-design-center). PCR plates (both 96-well plates and 386-well plates) were loaded using the Biomek FX liquid handling robot (Beckman Coulter) and the reactions [10 ng cDNA, 0.1 µM UPL probe, 0.2 µM forward primer, 0.2 µM reverse primer and 5 µL Luna[®] Universal Probe qPCR Master Mix (Cat: M3004E, New England Biolabs)] were amplified using the Prism7900HT sequence detection system (Applied Biosystems) and analyzed using sequence detection systems v2.4 software. Regarding the cells treated with FICZ only, gene expression values were normalized to glyceraldehyde-3-phosphate dehydrogenase (GAPDH) as housekeeping gene. Sequences of the primers are the following.

GAPDH, F: AGCCACATCGCTCAGACAC, R: GCCCAATACGACCAAATCC probe: #60. Claudin-3 (CLD-3), F: AACCTGCATGGACTGTGAAA, R: GGTCAAGTATTGGCGTCAC, probe: #50. Occludin (OCLN), F: AGGAACCGAGAGCCAGG, R: TTGAGCAATGCCCTTAGCTT, probe: #84. Zona occludence-1 (ZO-1), F: TGCATGATGATCGTCTGTCC, R: AAGTGTGTCTACTGTCCGTCTAT, probe:#01.

Relative expression was calculated using the $\Delta\Delta CT$ method as follows:

$$\text{Relative expression: \% relative expression} = 100 * (2^{-\Delta\Delta CT})$$

Where: $\Delta\Delta CT = \Delta Ct (\text{Target sample}) - \Delta Ct (\text{Calibrator sample})$

And: $\Delta CT = Ct (\text{Target gene}) - Ct (\text{Housekeeping gene})$

2.6. Protein extraction

Total protein was extracted using Radioimmunoprecipitation Assay (RIPA) Buffer Lysis and Extraction Buffer (Cat: 89900, Thermo Fisher Scientific). Cells were washed with cold PBS and incubated with RIPA buffer on ice for 30 min. Following this, cells were collected and centrifuged for 10 min at 14,000xg at 4°C, after which the protein lysate was aspirated.

2.7. Bradford and BCA assays

Protein concentrations were determined using either Bradford or Bicinchoninic Acid (BCA) assays. Samples in RIPA buffer were diluted 1:50 with Bradford Reagent (Cat: 5000205 Bio-Rad) or BCA (Cat: 23227 Thermo Fisher Scientific) in a 96-microtiter plate in triplicate. Absorbance was measured at wavelength 595 nm (reference: 450 nm) using a microplate reader and compared to a standard curve generated from dilutions of a known Bovine Serum Albumin (BSA) (Bio-Rad or Thermo Fisher Scientific) standard (0.125, 0.25, 0.5, 0.75, 1.0, 1.5, and 2.0 mg/mL).

2.8. Western blotting

Protein lysates were prepared in 4x Laemmli Sample Buffer (Cat: 1610747 Bio-Rad) with 10% 2-mercaptoethanol (Cat: M6250, Sigma-Aldrich Co Ltd) and boiled (5–10 min, 95°C). Lysates (30 µg) were separated on 8%, 10%, or 12% self-made sodium dodecyl sulfate-polyacrylamide gel electrophoresis (SDS-PAGE). Proteins

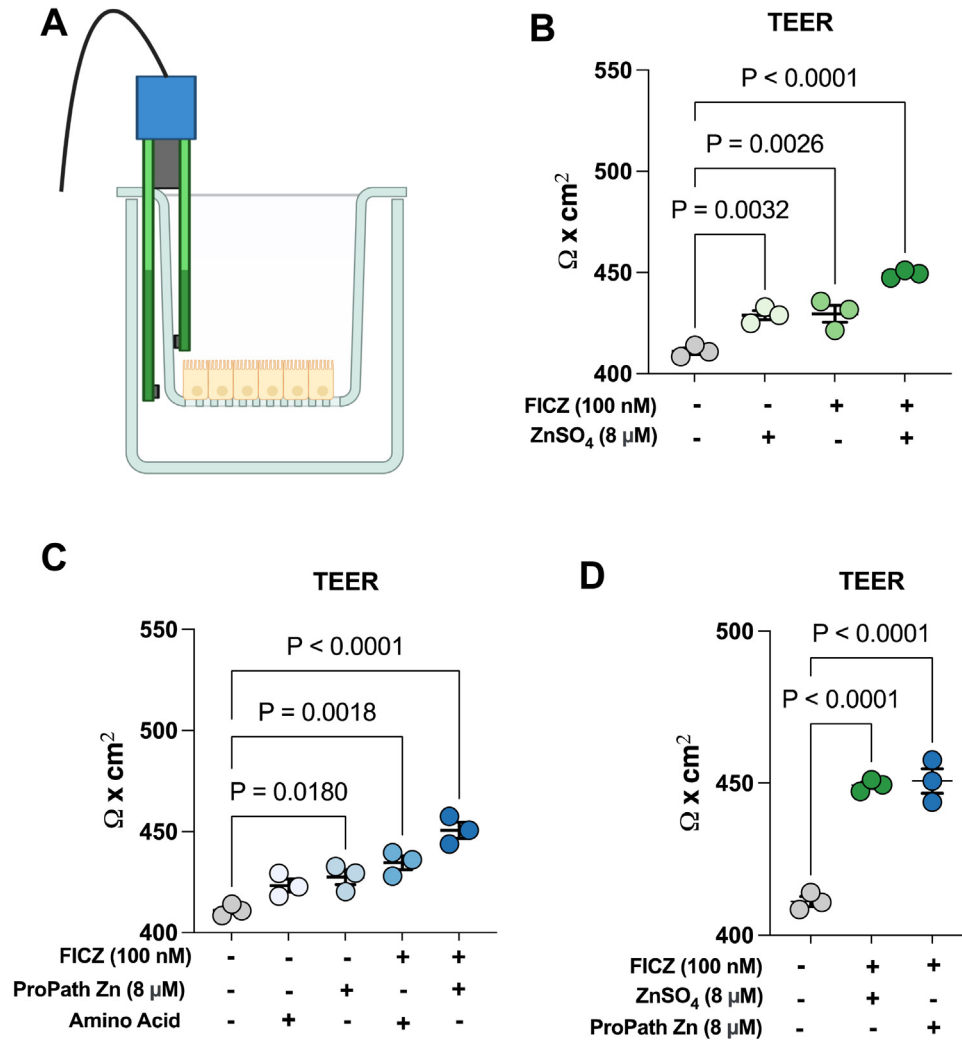


Fig. 1. FICZ and two different zinc compounds improve the trans-epithelial electrical resistance. (A) Caco-2 cells were grown to an epithelium in a Transwell® system. (B) TEER across Caco-2 cell epithelium kept in media with 0 or 8 μM ZnSO₄ and/or 100 nM FICZ. (C) TEER across Caco-2 cell epithelium kept in media with 0 or 8 μM ProPath® Zn and/or 100 nM FICZ. 'Amino Acids' is the amino acid component of ProPath without the zinc added. (D) Comparison of TEER across Caco-2 cell epithelium kept in media with either with 100 nM FICZ in combination with 8 μM ZnSO₄ or ProPath® Zn. Statistical analysis of the data was performed using two-way ANOVA followed by either Tukey's multiple comparison tests. Data are means ± SEM from three independent experiments (n = 3) with results from the experimental repeats shown. Significant differences between treatments are indicated by the P-values. Panel A was generated using Biorender.

were transferred onto nitrocellulose membranes [Cat: 10600002, GE Healthcare Life Sciences] at 100 V for 1 h, employing transfer buffer (25 mM Tris, 192 mM glycine, 10% methanol). After electrophoresis, membranes were blocked by incubation in 5% (w/v) bovine serum albumin (BSA)/Tris-buffered saline [TBS (50 mM Tris-HCl pH 7.5, 150 mM NaCl)] and 0.05% (v/v) TWEEN-20 [TBST (1 h, RT)]. Membranes were incubated with primary antibodies diluted in 5% BSA/TBST (20 h, 4°C), followed by horseradish peroxidase (HRP)-linked secondary antibodies diluted in 5% BSA/TBST (1 h, RT). Zona occludence-1 (ZO-1) rabbit antibody (Cell Signalling Technology, 13663) was diluted at a ratio of 1:800 for its application in the experiment. Membranes were washed three times with TBST between each step. Membranes were treated with enhanced chemiluminescence (ECL) Western Blotting Detection Reagent (Cat: RPN2106 GE Healthcare Life Sciences) and visualised on X-ray film (GE Healthcare Life Sciences) using a film imager.

2.9. Membrane stripping

Immunoblots were washed with TBST, with each wash lasting 5 min. Subsequently, the membranes were incubated in stripping

buffer (Cat: 21059, Thermo Fisher) for 18 min at room temperature, followed by an additional wash with TBST for 10 min at 21°C. To prepare for subsequent antibody incubation, the membranes were blocked with 5% (v/v) BSA/TBST (1 h). This process was carried out before proceeding with additional steps as outlined in Section 4.8 of the Western blotting protocol.

2.10. Total zinc determination

Inductively coupled plasma mass spectrometry (ICP-MS) was used for determining the total zinc content of both the two sources of zinc and Caco-2 cells. The two sources of zinc were dissolved in Milli Q-water to achieve a concentration of 1 mg/mL. Cells or chemicals were lysed in 1 mL 50m M Suprapur NaOH (VWR International) for 2 h. Samples were diluted with 400 μL trace element grade 65-69% nitric acid (Merck) and 100 μL H₂O₂ (Merck), before digestion with lid overnight at 60°C, then samples were diluted by adding 6 mL Milli Q-water. The zinc concentrations determined through ICP-MS was carried out using a NexIon 350 D (Perkin Elmer) mass spectrometer in the London Metallomics Fa-

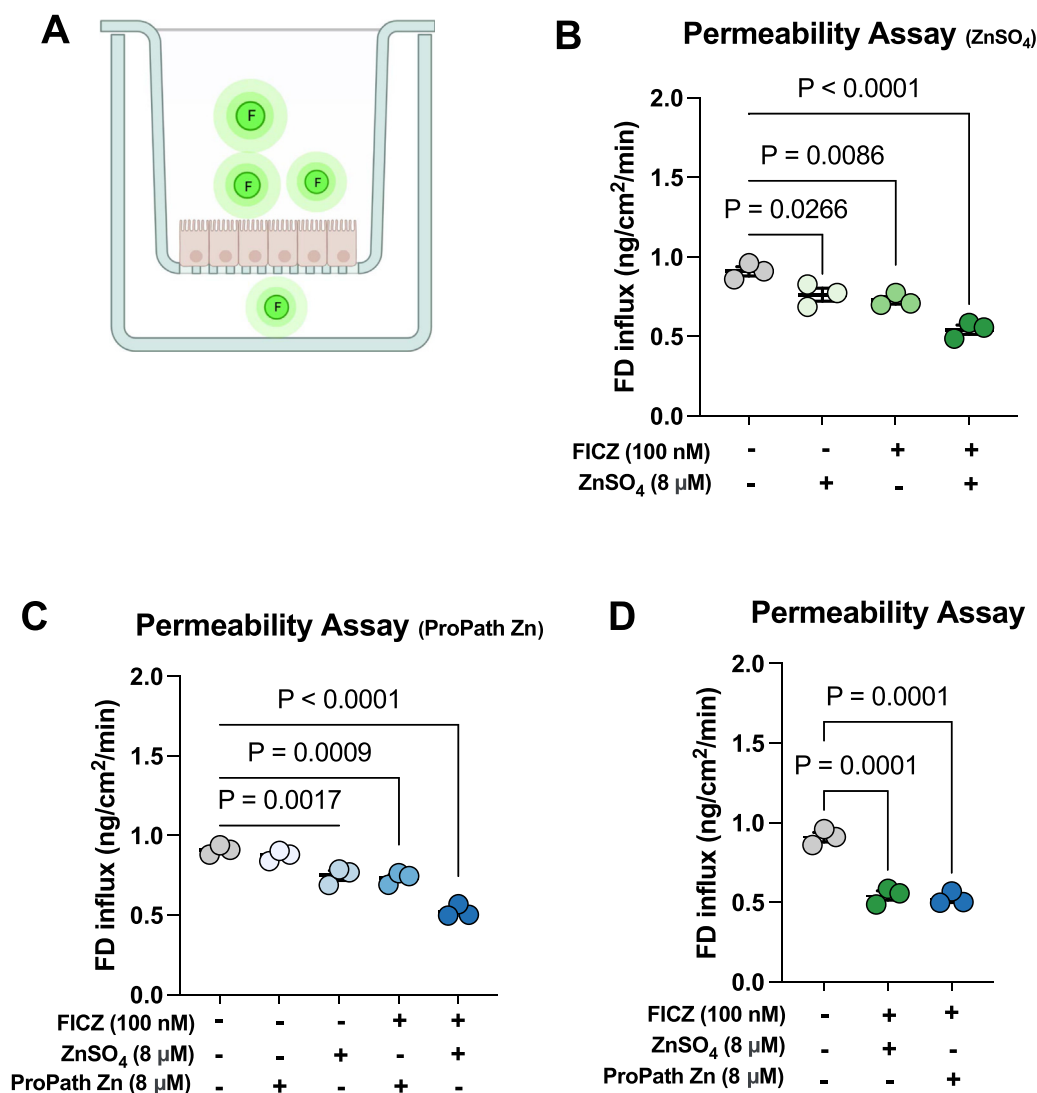


Fig. 2. Both FICZ and two different zinc compounds reduce the permeability of the Caco-2 epithelium. (A) Caco-2 cells were grown to an epithelium in a Transwell® system. At the start of the experiment, the medium in the apical compartment was replaced with MEM containing FITC-dextran 4000 (Merck) together with (B) 0 or 8 µM ZnSO₄ (C) or ProPath® Zn and/or 100 nM FICZ. 'Amino Acids' is the amino acid component of ProPath without the zinc added. Permeability was measured by sampling the medium in the basal compartment and measurement of FITC fluorescence over 24 h. (D) Comparison of the permeability across Caco-2 cell epithelium kept in media with 8 µM ZnSO₄ or ProPath® Zn and/or 100 nM FICZ. Statistical analysis of the data was performed using two-way ANOVA (B and C) or one-way ANOVA (D) followed by either Tukey's multiple comparison tests. Data are means ± SEM from three independent experiments ($n = 3$) with results from the experimental repeats shown. Significant differences between treatments are indicated by the P-values.

cility. As for cells, the total zinc content was normalized to protein content which was measured by BCA assays (see 4.7).

2.11. Cytosolic free Zn²⁺ quantification

After incubation with 1 µM FluoZin-3AM for 15–30 min at room temperature, cells were washed and incubated in Heps-buffered Hanks' balanced salt solution (HHBSS) for another 15 min at 21°C before readings were taken. Fluorescence was measured with 492 nm excitation and 517 nm emission in a fluorescence plate reader (F). 5 µM pyrithione together with 20 µM ZnCl₂ were used to treat cells for 15 min to obtain the maximum fluorescence reading (F_{max}), and 100 µM N, N, N', N'-tetrakis (2-pyridylmethyl) ethylenediamine (TPEN) for 15 min for the minimum fluorescence reading (F_{min}). Concentration of free intracellular free Zn²⁺ was calculated using the following equation:

$$[\text{Zn}^{2+}] = K_d * (F - F_{\text{min}}) / (F_{\text{max}} - F)$$

where K_d is the zinc dissociation constant of the probe (8.9 nM) (ThermoFisher Scientific).

2.12. The transepithelial electricity resistance measurement & permeability assay

Caco-2 cells (1×10^5) were grown on 0.336 cm² Transwell inserts (Cat: 655090, Greiner Bio-One Ltd). Transepithelial electrical resistance (TEER) was monitored daily using an epithelial tissue volt ohmmeter (EVOMX) with STX-2 chopsticks (World Precision Instruments). TEER measurements were calculated in ohms*cm² after subtracting the blank value for the membrane insert. The same inserts were employed for intestinal permeability assays. Fluorescein isothiocyanate (FITC)-dextran 4000 (Merck), 300 µL of 1 mg/mL solution was put in the apical compartment and 500 µL of the phenol red-free MEM (Cat: M3024, Merck). At 4, 8, 12, and 24 h, 100 µL of basolateral medium was collected for measurement by fluorometry (excitation, 475 nm; emission, 530 nm). After each

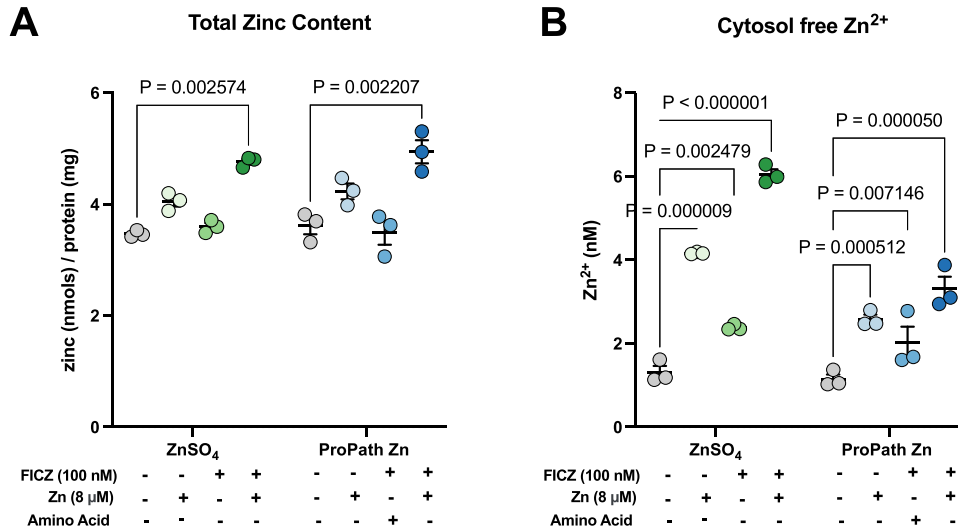


Fig. 3. FICZ treatment increases the total zinc content and intracellular free Zn²⁺ concentrations. (A) Total zinc content (measured by ICP-MS and normalised to protein content) or (B) free intracellular Zn²⁺ concentrations (measured with FluoZin-3AM probe) in Caco-2 cells following incubation with media containing 0 or 8 μM ZnSO₄ or ProPath[®] Zn and/or 100 nM FICZ for 24 h. “Amino Acids” is the amino acid component of ProPath without the zinc added. Statistical analysis of the data was performed using two-way ANOVA followed by either Tukey’s multiple comparison tests. Data are means ± SEM from three independent experiments (*n* = 3) with results from the experimental repeats shown. Significant differences between treatments are indicated by the *P*-values.

collection, 100 μL of fresh medium was added to replace the removed volume. Serial dilutions of FITC-dextran in medium were used to calculate a standard curve.

3. Results

Trans-epithelial electrical resistance (TEER) is widely used to evaluate barrier function of *in vitro* epithelia [30]. Caco-2 cells were seeded on the inserts to mimic the gut barrier (Figure 1A), and TEER was measured after 24 h of treatment. FICZ is a high-affinity AHR agonist with a *K_d* value of 0.07 nM [31]. However, other studies which made use of 500 nM FICZ, also saw the FICZ-AHR pathway attenuate the inflammation response and modulate the cell growth homeostasis in the rat [32,33], meaning that 500 nM FICZ protects. In the present study, we treated Caco-2 cells with 100 nM FICZ. We found previously that a much lower concentration of 10 nM has qualitatively the same effect on Caco-2 epithelial permeability but 100 nM produces a more robust response [14]. We tested the effects of FICZ in presence or absence of 8 μM zinc [14,34], which was the zinc concentration in the complete cell culture medium (with FBS) (8.04 ± 0.13 μM, *N* = 3).

In the presence of 8 μM ZnSO₄ or 100 nM FICZ, TEER was higher compared to the un-supplemented control (Figure 1B). Notably, the highest TEER was observed in the conditions where addition of 100 nM FICZ was combined with 8 μM zinc either as ZnSO₄ (Figure 1B) or ProPath[®] Zn (Figure 1C) with no difference in efficacy between the two zinc sources (Figure 1D). FICZ in combination with the amino acid component of ProPath (2.8 μM DL-lysine and 2.8 μM DL-glutamate) without the zinc also increased TEER, but to a smaller extent than in the presence of 8 μM ProPath[®] Zn (Figure 1C). However, the amino acid component of ProPath[®] alone had a small but significant effect on TEER (Figure 1C).

Permeability of the epithelium was assessed using fluorescent FITC-Dextran 4 K (FD-4) with the Transwell[®] system [35]. Caco-2 cells were seeded on the insert with FD-4 in the apical chamber, and FITC fluorescence in the medium from the basement chamber was measured using a microplate reader (Figure 2A). In the absence of treatment with FICZ and/or zinc, the FD-4 influx was about 0.9 ng/cm/min (Figures 2B and C). Treatment with 8 μM

ZnSO₄ or 100 nM FICZ slightly reduced FD-4 influx compared with the control (Figure 2B). However, the combination of 8 μM ZnSO₄ and 100 nM FICZ had a substantial positive effect in attenuating the increase of FD-4 influx, reducing it to about half of that of the control (Figure 2B). Addition of the amino acid mixture with the same composition as that in ProPath[®] Zn did not affect FD-4 permeability (Figure 2C). Addition of either 8 μM ProPath[®] Zn or with FICZ together with the amino acid components of ProPath[®] but without zinc had a small but significant ability to reduce permeability (Figure 2C). In contrast, a combination treatment with 8 μM ProPath[®] Zn and 100 nM FICZ reduced FD-4 permeability substantially (Figure 2C). The efficacies of the two sources of zinc, ProPath[®] Zn and ZnSO₄, in reducing transepithelial permeability in the presence of FICZ were almost identical (Figure 2D).

Treatment with either 8 μM ZnSO₄ or 8 μM ProPath[®] Zn in combination with 100 nM FICZ increased the total cellular zinc content compared with the controls (untreated and amino acids without added zinc) and compared with zinc only treatment from either source (Figure 3A). This observation is consistent with our recent findings that activation of AHR with FICZ increases expression of zinc importers in Caco-2 cells [12]. There was no significant difference in the total zinc content between the ZnSO₄ and ProPath[®] Zn treatments (Figure 3A). We also measured the free cytosolic Zn²⁺ concentration in Caco-2 cells and found that treatment with 8 μM zinc either from ZnSO₄ or ProPath[®] Zn increased cytosolic free Zn²⁺ concentrations (Figure 3B). Like with total zinc uptake in cells, adding FICZ to the medium further increased cellular free Zn²⁺ concentrations. However, the free Zn²⁺ concentrations in cells treated with ProPath[®] were lower than those in cells treated with ZnSO₄ (*P* < .01, Figure 3D). This difference might be explained by an increased uptake of the two amino acids along with zinc, increasing the cytosolic buffering capacity for Zn²⁺.

Next, we investigated if the changes in transepithelial resistance and permeability were associated with changes in expression of genes for proteins making up the tight junctions. As a control for AHR activation, we measured mRNA for *CYP1A1* after 24 h treatment of Caco-2 cells with 100 nM FICZ or 8 μM ZnSO₄. FICZ treatment resulted in strong induction of *CYP1A1*, indicating that FICZ activated AHR in our experimental system (Figure 4A). The pres-

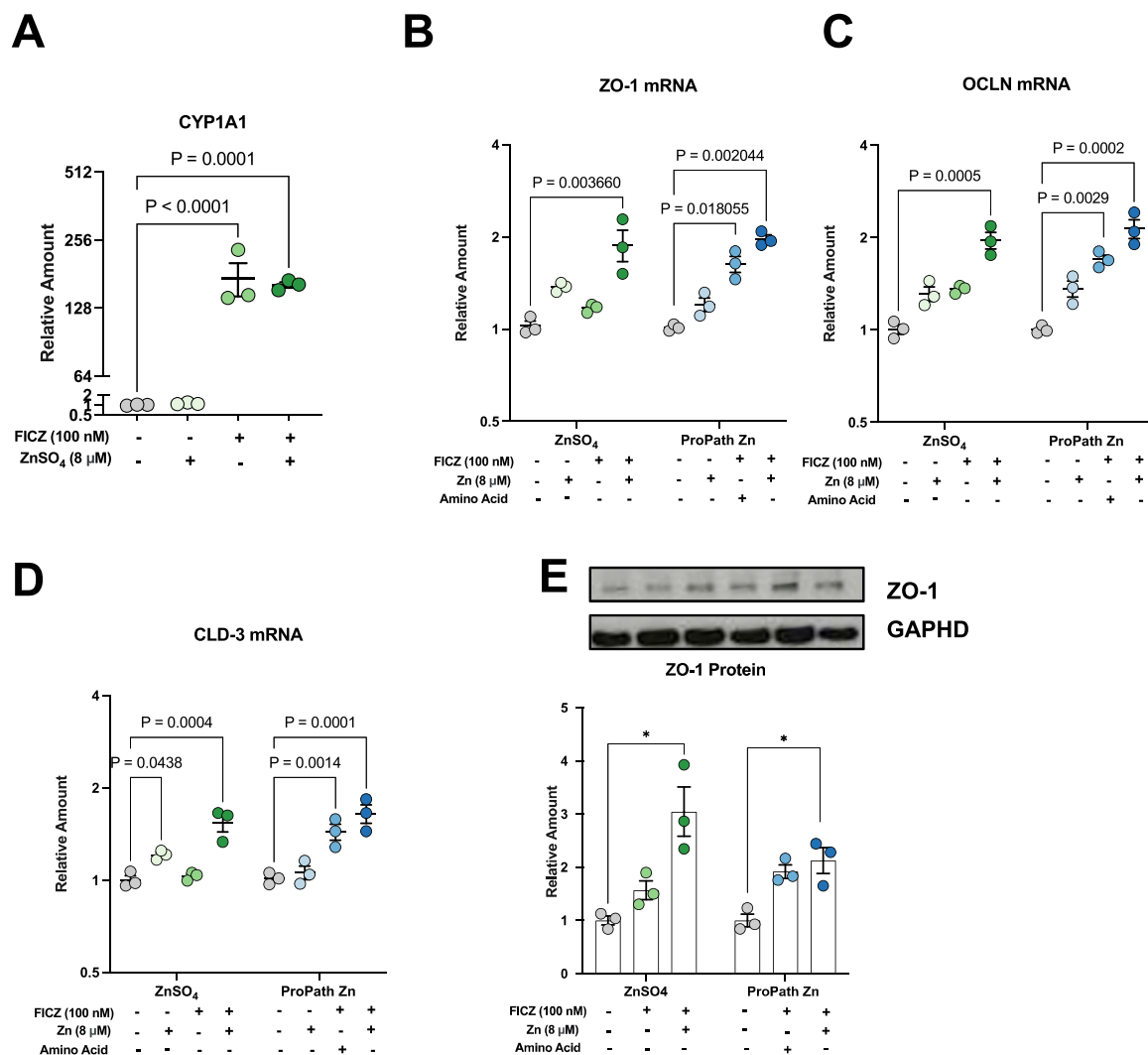


Fig. 4. Both FICZ and the two zinc compounds increase the expression of the TJ-related genes and protein. (A) *CYP1A1* mRNA following 24 h treatment of Caco-2 cells with 100 nM FICZ and/or 8 μM ZnSO₄ indicative of AHR activation. Expression of mRNA for tight junction proteins including (B) ZO-1, (C) OCLN and (D) CLD-3 in Caco-2 cells treated with 0 or 8 μM ZnSO₄ or ProPath[®] Zn and/or 100 nM FICZ for 24 h. (E) Abundance of tight junction protein, ZO-1, as measured by western blot, in Caco-2 cells treated with 0 or 8 μM ZnSO₄ or ProPath[®] Zn and/or 100 nM FICZ for 24 h. Western blot membrane with one repeat of the experiment is shown. See supplementary material 1 for the uncropped Western Blot. 'Amino Acids' is the amino acid component of ProPath without the zinc added. Statistical analysis of the data was performed using two-way ANOVA followed by Tukey's multiple comparison tests. Data are means ± SEM from three independent experiments ($n = 3$) with results from the experimental repeats shown. Significant differences between treatments are indicated by the *P*-values.

ence or absence of 8 μM ZnSO₄ did not influence *CYP1A1* mRNA expression (Figure 4A). Caco-2 cells were treated with 8 μM ZnSO₄ or ProPath[®] Zn with or without FICZ and mRNA for ZO-1, OCLN, and CLD-3 was measured along with protein levels of ZO-1. Treatment with FICZ in combination with either ZnSO₄ or ProPath[®] Zn increased mRNA levels of ZO-1, OCLN, and CLD-3 (Figure 4B, C, and D; Supplementary Material 1). Interestingly, the amino acid component of ProPath[®] Zn (without added zinc) also significantly increased the expression of these three genes when given to the cells in combination with FICZ (Figure 4B, C, and D). ProPath[®] Zn combined with FICZ only showed a significant increase compared with the amino acids and FICZ treatment for CLD-3. In the case of ZO-1 protein abundance, both sources of zinc in combination with FICZ exhibited a significant increase (Figure 4E).

4. Discussion

There is a strong interest in zinc chelates (sometimes referred to as "organic zinc") as nutritional supplements for animals and

human, and some studies have indicated that amino acid chelates of zinc are better absorbed than inorganic forms [36–38]. In their assessment of the efficacy and safety of ProPath[®] Zn for use in animal feeds, the European Food Safety Authority (EFSA) concluded that the additive can satisfy the zinc requirement of chicken and they extended that conclusion to all animal species [24]. In the present study we found that ProPath[®] Zn is absorbed as efficiently by a human Caco-2 cell epithelium as ZnSO₄, which is generally considered the most bioavailable inorganic zinc source.

Glover and Hogstrand [25] found that histidine, cysteine and taurine chelates of zinc had distinct modifying actions upon quantitative and qualitative zinc absorption and body distribution, compared to ZnSO₄. They also found evidence for a Zn(His)₂-mediated pathway for intestinal zinc uptake [39]. These observations suggest that bioavailability of a zinc chelate does not necessarily mean that it is utilized in the same way as inorganic zinc sources. We recently discovered that zinc (as zinc sulfate or zinc carbonate) and the AHR interact to reduce paracellular permeability of the intestinal epithelium, thereby protecting against IBD [14]. In the present

study we compared the efficacy of ProPath® Zn with ZnSO₄ in promoting the barrier function of a Caco-2 cell epithelium and found no difference between the two sources of zinc. Activation of AHR was as effective in improving the effect of ProPath® Zn on epithelial permeability as it was in combination with ZnSO₄. AHR agonists act on the epithelium at least in part by stimulating expression of zinc importers of the ZIP (SLC39) family [14], which mediate uptake of Zn²⁺ ions [39]. Thus, the ability of AHR activation to increase uptake of zinc from ProPath® Zn and thereby improving epithelial barrier function implies that zinc from ProPath® Zn is absorbed as Zn²⁺. It was somewhat surprising to find that treatment of Caco-2 cells with ProPath® Zn resulted in lower intracellular free Zn²⁺ concentrations compared with treatments with ZnSO₄ at the same concentrations. This might be explained by a higher amino acid uptake in the ProPath® Zn treatments, resulting in higher intracellular chelating capacity for zinc. Regardless of this, ProPath® Zn was as efficacious as ZnSO₄ in stimulating expression of genes for TJ proteins. Therefore, at least in the Caco-2 intestinal epithelium model, ProPath® Zn is utilized in the same way as ZnSO₄.

TJs are only one part of the barrier function of the intestine [40]. Intestinal stem cell proliferation and differentiation can also affect the barrier function [41]. There is evidence that zinc and AHR activation have opposite functions in the cell proliferation since Zn activates the β -catenin/Wnt pathway which is inhibited by AHR [13,42]. Thus, exploring the mechanism of both Zn and AHR in stem cell proliferation and differentiation could provide more detailed information of their functions in the gut barrier. Besides, AHR is well-studied in the mucosal immunity [43] and it works as the gatekeeper to maintain the intestinal immune functions through being activated by AHR ligands. Both depletion of AHR and constitutive expression of the AHR target gene, *Cyp1a1*, in mice cause the loss of AHR-dependent type 3 innate lymphoid cells and T helper 17 cells, increasing susceptibility to enteric infection [11]. Zinc is important for the immune system [44], but the mechanisms involved are only partially known. B cells deficient in cytosolic free Zn²⁺ showed elevated protein phosphatase activity and reduced phosphorylation of downstream signalling molecules, including SYK, PLC γ 2 and ERK, from pre-B cell and B cell receptors, resulting in a block in B cell development [45]. Although not investigated in that study it is known that Zn²⁺ is a potent inhibitor of many protein tyrosine phosphatases (PTPs) [46–48]. Using molecular dynamics simulations, metadynamics, and quantum chemical calculations in combination with experimental investigations it was found that Zn²⁺ inhibits PTPs by reversibly binding to the active site which is conserved among PTPs [49]. Also, Zn can mediate I κ B kinase activity to decrease the activation of Nuclear Factor Kappa B (NF κ B) that serves as a pivotal mediator of inflammatory responses [50,51]. Thus, understanding the interplay between AHR activation and zinc status provides insights into the intricate regulation of intestinal immunity.

There are some limitations to the present study. In our previous work [14] we were able to show in mice, human ileum organoids, and in Caco-2 cells that the direct effects of AHR on permeability of the intestinal epithelial layer are primarily mediated by transcriptional upregulation of zinc importers of the SLC39A family, which enhances zinc influx. The increase of free cytosolic Zn²⁺ in the epithelial cells is then increasing abundance of tight junction proteins by inhibition of the NF κ B pathway resulting in their increased expression, and by attenuated degradation of tight junction proteins by inhibition of calpain. In future research, it would be beneficial to make AHR knockout Caco-2 cells to verify that the same mechanism applies also when cells are presented with zinc as an amino acid chelate. In the experiments of the present study, we did not confirm differentiation of the Caco-2 cell epithelium

using differentiation markers. The protocol we used reproducibly produces a differentiated epithelium [29] and it was therefore considered not necessary to confirm differentiation with markers such as Divalent Metal Transporter-1 (DMT1) protein and mRNA expression although ultimately this would have been beneficial.

5. Conclusions

The results highlight the beneficial influence of two sources of bioavailable zinc on gut health, particularly emphasizing the enhancement of Caco-2 epithelium barrier function through AHR activation using a physiologically relevant ligand, in combination with two distinct zinc sources. The observed rise in cellular zinc concentrations, intracellular free Zn²⁺, and increased mRNA expression of tight junction proteins by AHR activation offers valuable insights for innovative therapeutic strategies designed to prevent and potentially treat inflammatory bowel disease (IBD). Further investigation into these mechanisms holds the potential to pave the way for targeted interventions, ultimately improving overall gastrointestinal health.

Declaration of competing interest

The authors declare the following financial interests/personal relationships which may be considered as potential competing interests:

Christer Hogstrand reports financial support was provided by Guts UK. Christer Hogstrand reports financial support was provided by Zinpro Corp. Wolfgang Maret reports financial support was provided by Wellcome Trust. ProPath Zn and the amino acid complement of this product (ProPath) was gifted to the Corresponding Author by ZinPro Performance Minerals. If there are other authors, they declare that they have no known competing financial interests or personal relationships that could have appeared to influence the work reported in this paper.

CRedit authorship contribution statement

Xiuchuan Hu: Writing – original draft, Validation, Methodology, Investigation, Formal analysis, Data curation. **Rui Wang:** Investigation, Formal analysis. **Peter Kille:** Writing – review & editing, Funding acquisition, Conceptualization. **Wolfgang Maret:** Writing – review & editing, Supervision, Methodology, Funding acquisition, Conceptualization. **Christer Hogstrand:** Writing – review & editing, Supervision, Resources, Project administration, Funding acquisition, Conceptualization.

Data availability statement

The dataset in the current study is available from the corresponding author upon reasonable request.

Funding

The authors wish to thank Prof. Paul Sharp at the King's College London, for the Caco-2 cell line, and Mr. Alexander Griffiths at London Metallomics Facility (LMF) for metal analysis by ICP-MS. This work was supported by grants from Guts UK (DGN2019_02 to C.H.), ZinPro Performance Minerals (1117612 to C.H.). X.H. was supported by a studentship from the Chinese Scholarship Council and King's College London. Metal analyses were performed in the LMF, which was funded by the Wellcome Trust (202902/Z/16/Z to Prof. Phil Blower, W.M. and C.H.). Analysis of gene expression by qPCR was carried out in King's College London Genomics Centre.

Supplementary materials

Supplementary material associated with this article can be found, in the online version, at doi:10.1016/j.jnutbio.2025.109909.

References

- [1] Barbara G, Barbaro MR, Fuschi D, Palombo M, Falangone F, Cremon C, et al. Inflammatory and microbiota-related regulation of the intestinal epithelial barrier. *Front Nutr* 2021;8:718356.
- [2] Groschwitz KR, Hogan SP. Intestinal barrier function: molecular regulation and disease pathogenesis. *J Allergy Clin Immunol* 2009;124:3–20 quiz 1–2.
- [3] Pastorelli L, De Salvo C, Mercado JR, Vecchi M, Pizarro TT. Central role of the gut epithelial barrier in the pathogenesis of chronic intestinal inflammation: lessons learned from animal models and human genetics. *Front Immunol* 2013;4:280.
- [4] Nebert DW. Aryl hydrocarbon receptor (AHR): "pioneer member" of the basic-helix/loop/helix per-Arnt-sim (bHLH/PAS) family of "sensors" of foreign and endogenous signals. *Prog Lipid Res* 2017;67:38–57.
- [5] Hubbard TD, Murray IA, Nichols RG, Cassel K, Podolsky M, Kuzu G, et al. Dietary broccoli impacts microbial community structure and attenuates chemically induced colitis in mice in an Ah receptor dependent manner. *J Funct Foods* 2017;37:685–98.
- [6] Rothhammer V, Quintana FJ. The aryl hydrocarbon receptor: an environmental sensor integrating immune responses in health and disease. *Nat Rev Immunol* 2019;19:184–97.
- [7] Cervantes-Barragan L, Chai JN, Tianero MD, Di Luccia B, Ahern PP, Merriman J, et al. *Lactobacillus reuteri* induces gut intraepithelial CD4⁺CD8 α ⁺T cells. *Science* 2017;357:806–10.
- [8] Aoki R, Aoki-Yoshida A, Suzuki C, Takayama Y. Indole-3-Pyruvic acid, an aryl hydrocarbon receptor activator, suppresses experimental colitis in mice. *The Journal of Immunology* 2018;201:3683–93.
- [9] Gomez de Agüero M, Ganal-Vonarburg SC, Fuhrer T, Rupp S, Uchimura Y, Li H, et al. The maternal microbiota drives early postnatal innate immune development. *Science* 2016;351:1296–302.
- [10] Lamas B, Richard ML, Leducq V, Pham HP, Michel ML, Da Costa G, et al. CARD9 impacts colitis by altering gut microbiota metabolism of tryptophan into aryl hydrocarbon receptor ligands. *Nat Med* 2016;22:598–605.
- [11] Schiering C, Wincent E, Metidji A, Iseppon A, Li Y, Potocnik AJ, et al. Feedback control of AHR signalling regulates intestinal immunity. *Nature* 2017;542:242–5.
- [12] Qiu J, Zhou L. Aryl hydrocarbon receptor promotes ROR gamma t(+) Group 3 ILCs and controls intestinal immunity and inflammation. *Semin Immunopathol* 2013;35:657–70.
- [13] Metidji A, Omenetti S, Crotta S, Li Y, Nye E, Ross E, et al. The environmental sensor AHR protects from inflammatory damage by maintaining intestinal stem cell homeostasis and barrier integrity. *Immunity* 2018;49:353–62.
- [14] Hu X, Xiao W, Lei Y, Green A, Lee X, Maradana MR, et al. Aryl hydrocarbon receptor utilises cellular zinc signals to maintain the gut epithelial barrier. *Nature Communications* 2023;14:5431.
- [15] Shah K, Maradana MR, Joaquina Delàs M, Metidji A, Graelmann F, Llorian M, et al. Cell-intrinsic Aryl hydrocarbon receptor signalling is required for the resolution of injury-induced colonic stem cells. *Nat Commun* 2022;13:1827.
- [16] Park JH, Lee JM, Lee EJ, Hwang WB, Kim DJ. Indole-3-carbinol promotes goblet-cell differentiation regulating wnt and notch signaling pathways AhR-dependently. *Mol Cells* 2018;41:290–300.
- [17] Yang S, Yu M. Role of goblet cells in intestinal barrier and mucosal immunity. *J Inflamm Res* 2021;14:3171–83.
- [18] Hojyo S, Fukada T. Roles of zinc signaling in the immune system. *J Immunol Res* 2016;2016:6762343.
- [19] Ohashi W, Fukada T. Contribution of zinc and zinc transporters in the pathogenesis of inflammatory bowel diseases. *J Immunol Res* 2019;2019:8396878.
- [20] Bajait C, Thawani V. Role of zinc in pediatric diarrhea. *Indian J Pharmacol* 2011;43:232–5.
- [21] Maret W. Zinc in cellular regulation: the nature and significance of "Zinc signals". *Int J Mol Sci* 2017;18(11):2285.
- [22] Wessels I, Maywald M, Rink L. Zinc as a gatekeeper of immune function. *Nutrients* 2017;9(12):1286.
- [23] Bampidis V, Azimonti G, Bastos ML, Christensen H, Dusemund B, Kouba M, et al. Safety and efficacy of zinc chelates of lysine and glutamic acid as feed additive for all animal species. *Efsa j* 2019;17:e05782.
- [24] Bampidis V, Azimonti G, Bastos ML, Christensen H, et al., Additives EPo, Products or Substances used in Animal F Safety and efficacy of zinc chelates of lysine and glutamic acid as feed additive for all animal species. *Efsa J* 2019;17:e05782.
- [25] Glover CN, Hogstrand C. Amino acid modulation of *in vivo* intestinal zinc absorption in freshwater rainbow trout. *J Exp Biol* 2002;205:151–8.
- [26] Briske-Anderson MJ, Finley JW, Newman SM. The influence of culture time and passage number on the morphological and physiological development of Caco-2 cells. *Proc Soc Exp Biol Med* 1997;214:248–57.
- [27] Maares M, Haase H. A guide to Human zinc absorption: general overview and recent advances of *in vitro* intestinal models. *Nutrients* 2020;12:762.
- [28] GO Latunde-Dada, Kajarabille N, Rose S, Arafsha SM, Kose T, Aslam MF, et al. Content and availability of minerals in plant-based burgers compared with a meat burger. *Nutrients* 2023;15:2732.
- [29] Sharp P, Tandy S, Yamaji S, Tennant J, Williams M, Singh Srari SK. Rapid regulation of divalent metal transporter (DMT1) protein but not mRNA expression by non-haem iron in human intestinal Caco-2 cells. *FEBS Lett* 2002;510:71–6.
- [30] Srinivasan B, Kolli AR, Esch MB, Abaci HE, Shuler ML, Hickman JJ. TEER measurement techniques for *in vitro* barrier model systems. *J Lab Autom* 2015;20:107–26.
- [31] Rannug A, Rannug U, Rosenkranz HS, Winqvist L, Westerholm R, Agurell E, et al. Certain photooxidized derivatives of tryptophan bind with very high affinity to the Ah receptor and are likely to be endogenous signal substances. *J Biol Chem* 1987;262:15422–7.
- [32] Rannug A, Rannug U. The tryptophan derivative 6-formylindolo[3,2-b]carbazole, FICZ, a dynamic mediator of endogenous aryl hydrocarbon receptor signaling, balances cell growth and differentiation. *Crit Rev Toxicol* 2018;48:555–74.
- [33] Huang J, Wang Y, Zhou Y. Beneficial roles of the AhR ligand FICZ on the regenerative potentials of BMSCs and primed cartilage templates. *RSC Adv* 2022;12:11505–16.
- [34] Lawson R, Maret W, Hogstrand C. Prolonged stimulation of insulin release from MIN6 cells causes zinc depletion and loss of beta-cell markers. *J Trace Elem Med Biol* 2018;49:51–9.
- [35] Thomas A, Wang S, Sohrabi S, Orr C, He R, Shi W, et al. Characterization of vascular permeability using a biomimetic microfluidic blood vessel model. *Biomicrofluidics* 2017;11:024102.
- [36] Yu Y, Lu L, Li SF, Zhang LY, Luo XG. Organic zinc absorption by the intestine of broilers *in vivo*. *Br J Nutr* 2017;117:1086–94.
- [37] Yue M, Fang SL, Zhuo Z, Li DD, Feng J. Zinc glycine chelate absorption characteristics in Sprague Dawley rat. *J Anim Physiol Anim Nutr (Berl)* 2015;99:457–64.
- [38] Zhang L, Guo Q, Duan Y, Lin X, Ni H, Zhou C, et al. Comparison of the effects of inorganic or amino acid-chelated zinc on mouse myoblast growth *in vitro* and growth performance and carcass traits in growing-finishing pigs. *Front Nutr* 2022;9:857393.
- [39] Qiu A, Hogstrand C. Functional expression of a low-affinity zinc uptake transporter (FrZIP2) from pufferfish (*Takifugu rubripes*) in MDCK cells. *Biochem J* 2005;390:777–86.
- [40] Suzuki T. Regulation of the intestinal barrier by nutrients: the role of tight junctions. *Anim Sci J* 2020;91:e13357.
- [41] Umar S. Intestinal stem cells. *Curr Gastroenterol Rep* 2010;12:340–8.
- [42] Zhao J, Han J, Jiang J, Shi S, Ma X, Liu X, et al. The downregulation of wnt/ β -catenin signaling pathway is associated with zinc deficiency-induced proliferative deficit of C17.2 neural stem cells. *Brain Res* 2015;1615:61–70.
- [43] Lamas B, Natividad JM, Sokol H. Aryl hydrocarbon receptor and intestinal immunity. *Mucosal Immunol* 2018;11:1024–38.
- [44] Prasad AS. Zinc in human health: effect of zinc on immune cells. *Mol Med* 2008;14:353–7.
- [45] Anzilotti C, Swan DJ, Boisson B, Deobagkar-Lele M, Oliveira C, Chabosseau P, et al. An essential role for the Zn(2+) transporter ZIP7 in B cell development. *Nat Immunol* 2019;20:350–61.
- [46] Haase H, Maret W. Intracellular zinc fluctuations modulate protein tyrosine phosphatase activity in insulin/insulin-like growth factor-1 signaling. *Exp Cell Res* 2003;291:289–98.
- [47] Wilson M, Hogstrand C, Maret W. Picomolar concentrations of free zinc(II) ions regulate receptor protein-tyrosine phosphatase beta activity. *J Biol Chem* 2012;287:9322–6.
- [48] Plum LM, Brieger A, Engelhardt G, Hebel S, Nessel A, Arlt M, et al. PTEN-inhibition by zinc ions augments interleukin-2-mediated akt phosphorylation. *Metallomics* 2014;6:1277–87.
- [49] Bellomo E, Abro A, Hogstrand C, Maret W, Domene C. Role of zinc and magnesium ions in the modulation of phosphoryl transfer in protein tyrosine phosphatase 1B. *J Am Chem Soc* 2018;140:4446–54.
- [50] Liu T, Zhang L, Joo D, Sun SC. NF-kappaB signaling in inflammation. *Signal Transduct Target Ther* 2017;2:17023.
- [51] Liu MJ, Bao S, Galvez-Peralta M, Pyle CJ, Rudawsky AC, Pavlovicz RE, et al. ZIP8 regulates host defense through zinc-mediated inhibition of NF-kappaB. *Cell Rep* 2013;3:386–400.